
Applied Superconductivity:

Josephson Effect and Superconducting Electronics

**Manuscript to the Lectures during WS 2003/2004, WS 2005/2006, WS 2006/2007,
WS 2007/2008, WS 2008/2009, and WS 2009/2010**

Prof. Dr. Rudolf Gross

and

Dr. Achim Marx

Walther-Meißner-Institut
Bayerische Akademie der Wissenschaften
and

Lehrstuhl für Technische Physik (E23)
Technische Universität München

Walther-Meißner-Strasse 8
D-85748 Garching
Rudolf.Gross@wmi.badw.de

Contents

Preface	xxi
I Foundations of the Josephson Effect	1
1 Macroscopic Quantum Phenomena	3
1.1 The Macroscopic Quantum Model	3
1.1.1 Coherent Phenomena in Superconductivity	3
1.1.2 Macroscopic Quantum Currents in Superconductors	12
1.1.3 The London Equations	18
1.2 Flux Quantization	24
1.2.1 Flux and Fluxoid Quantization	26
1.2.2 Experimental Proof of Flux Quantization	28
1.2.3 Additional Topic: Rotating Superconductor	30
1.3 Josephson Effect	32
1.3.1 The Josephson Equations	33
1.3.2 Josephson Tunneling	37
2 JJs: The Zero Voltage State	43
2.1 Basic Properties of Lumped Josephson Junctions	44
2.1.1 The Lumped Josephson Junction	44
2.1.2 The Josephson Coupling Energy	45
2.1.3 The Superconducting State	47
2.1.4 The Josephson Inductance	49
2.1.5 Mechanical Analogs	49
2.2 Short Josephson Junctions	50
2.2.1 Quantum Interference Effects – Short Josephson Junction in an Applied Magnetic Field	50

2.2.2	The Fraunhofer Diffraction Pattern	54
2.2.3	Determination of the Maximum Josephson Current Density	58
2.2.4	Additional Topic: Direct Imaging of the Supercurrent Distribution	62
2.2.5	Additional Topic: Short Josephson Junctions: Energy Considerations	63
2.2.6	The Motion of Josephson Vortices	65
2.3	Long Josephson Junctions	68
2.3.1	The Stationary Sine-Gordon Equation	68
2.3.2	The Josephson Vortex	70
2.3.3	Junction Types and Boundary Conditions	73
2.3.4	Additional Topic: Josephson Current Density Distribution and Maximum Josephson Current	79
2.3.5	The Pendulum Analog	84
3	JJs: The Voltage State	89
3.1	The Basic Equation of the Lumped Josephson Junction	90
3.1.1	The Normal Current: Junction Resistance	90
3.1.2	The Displacement Current: Junction Capacitance	92
3.1.3	Characteristic Times and Frequencies	93
3.1.4	The Fluctuation Current	94
3.1.5	The Basic Junction Equation	96
3.2	The Resistively and Capacitively Shunted Junction Model	97
3.2.1	Underdamped and Overdamped Josephson Junctions	100
3.3	Response to Driving Sources	102
3.3.1	Response to a dc Current Source	102
3.3.2	Response to a dc Voltage Source	107
3.3.3	Response to ac Driving Sources	107
3.3.4	Photon-Assisted Tunneling	112
3.4	Additional Topic: Effect of Thermal Fluctuations	115
3.4.1	Underdamped Junctions: Reduction of I_c by Premature Switching	117
3.4.2	Overdamped Junctions: The Ambegaokar-Halperin Theory	118
3.5	Secondary Quantum Macroscopic Effects	122
3.5.1	Quantum Consequences of the Small Junction Capacitance	122

3.5.2	Limiting Cases: The Phase and Charge Regime	125
3.5.3	Coulomb and Flux Blockade	128
3.5.4	Coherent Charge and Phase States	130
3.5.5	Quantum Fluctuations	132
3.5.6	Macroscopic Quantum Tunneling	133
3.6	Voltage State of Extended Josephson Junctions	139
3.6.1	Negligible Screening Effects	139
3.6.2	The Time Dependent Sine-Gordon Equation	140
3.6.3	Solutions of the Time Dependent Sine-Gordon Equation	141
3.6.4	Additional Topic: Resonance Phenomena	144
II	Applications of the Josephson Effect	153
4	SQUIDS	157
4.1	The dc-SQUID	159
4.1.1	The Zero Voltage State	159
4.1.2	The Voltage State	164
4.1.3	Operation and Performance of dc-SQUIDS	168
4.1.4	Practical dc-SQUIDS	172
4.1.5	Read-Out Schemes	176
4.2	Additional Topic: The rf-SQUID	180
4.2.1	The Zero Voltage State	180
4.2.2	Operation and Performance of rf-SQUIDS	182
4.2.3	Practical rf-SQUIDS	186
4.3	Additional Topic: Other SQUID Configurations	188
4.3.1	The DROS	188
4.3.2	The SQIF	189
4.3.3	Cartwheel SQUID	189
4.4	Instruments Based on SQUIDS	191
4.4.1	Magnetometers	192
4.4.2	Gradiometers	194
4.4.3	Susceptometers	196

4.4.4	Voltmeters	197
4.4.5	Radiofrequency Amplifiers	198
4.5	Applications of SQUIDs	200
4.5.1	Biomagnetism	200
4.5.2	Nondestructive Evaluation	204
4.5.3	SQUID Microscopy	206
4.5.4	Gravity Wave Antennas and Gravity Gradiometers	208
4.5.5	Geophysics	210
5	Digital Electronics	215
5.1	Superconductivity and Digital Electronics	216
5.1.1	Historical development	217
5.1.2	Advantages and Disadvantages of Josephson Switching Devices	219
5.2	Voltage State Josephson Logic	222
5.2.1	Operation Principle and Switching Times	222
5.2.2	Power Dissipation	225
5.2.3	Switching Dynamics, Global Clock and Punchthrough	226
5.2.4	Josephson Logic Gates	228
5.2.5	Memory Cells	234
5.2.6	Microprocessors	236
5.2.7	Problems of Josephson Logic Gates	237
5.3	RSFQ Logic	239
5.3.1	Basic Components of RSFQ Circuits	241
5.3.2	Information in RSFQ Circuits	246
5.3.3	Basic Logic Gates	247
5.3.4	Timing and Power Supply	249
5.3.5	Maximum Speed	249
5.3.6	Power Dissipation	250
5.3.7	Prospects of RSFQ	250
5.3.8	Fabrication Technology	253
5.3.9	RSFQ Roadmap	254
5.4	Analog-to-Digital Converters	255
5.4.1	Additional Topic: Foundations of ADCs	256
5.4.2	The Comparator	261
5.4.3	The Aperture Time	263
5.4.4	Different Types of ADCs	264

6	The Josephson Voltage Standard	269
6.1	Voltage Standards	270
6.1.1	Standard Cells and Electrical Standards	270
6.1.2	Quantum Standards for Electrical Units	271
6.2	The Josephson Voltage Standard	274
6.2.1	Underlying Physics	274
6.2.2	Development of the Josephson Voltage Standard	274
6.2.3	Junction and Circuit Parameters for Series Arrays	279
6.3	Programmable Josephson Voltage Standard	281
6.3.1	Pulse Driven Josephson Arrays	283
7	Superconducting Photon and Particle Detectors	285
7.1	Superconducting Microwave Detectors: Heterodyne Receivers	286
7.1.1	Noise Equivalent Power and Noise Temperature	286
7.1.2	Operation Principle of Mixers	287
7.1.3	Noise Temperature of Heterodyne Receivers	290
7.1.4	SIS Quasiparticle Mixers	292
7.1.5	Josephson Mixers	296
7.2	Superconducting Microwave Detectors: Direct Detectors	297
7.2.1	NEP of Direct Detectors	298
7.3	Thermal Detectors	300
7.3.1	Principle of Thermal Detection	300
7.3.2	Bolometers	302
7.3.3	Antenna-Coupled Microbolometers	307
7.4	Superconducting Particle and Single Photon Detectors	314
7.4.1	Thermal Photon and Particle Detectors: Microcalorimeters	314
7.4.2	Superconducting Tunnel Junction Photon and Particle Detectors	318
7.5	Other Detectors	328
8	Microwave Applications	329
8.1	High Frequency Properties of Superconductors	330
8.1.1	The Two-Fluid Model	330
8.1.2	The Surface Impedance	333
8.2	Superconducting Resonators and Filters	336
8.3	Superconducting Microwave Sources	337

9 Superconducting Quantum Bits	339
9.1 Quantum Bits and Quantum Computers	341
9.1.1 Quantum Bits	341
9.1.2 Quantum Computing	343
9.1.3 Quantum Error Correction	346
9.1.4 What are the Problems?	348
9.2 Implementation of Quantum Bits	349
9.3 Why Superconducting Qubits	352
9.3.1 Superconducting Island with Leads	352
III Anhang	355
A The Josephson Equations	357
B Imaging of the Maximum Josephson Current Density	361
C Numerical Iteration Method for the Calculation of the Josephson Current Distribution	363
D Photon Noise	365
I Power of Blackbody Radiation	365
II Noise Equivalent Power	367
E Qubits	369
I What is a quantum bit ?	369
I.1 Single-Qubit Systems	369
I.2 The spin-1/2 system	371
I.3 Two-Qubit Systems	372
II Entanglement	373
III Qubit Operations	375
III.1 Unitarity	375
III.2 Single Qubit Operations	375
III.3 Two Qubit Operations	376
IV Quantum Logic Gates	377
IV.1 Single-Bit Gates	377
IV.2 Two Bit Gates	379
V The No-Cloning Theorem	384
VI Quantum Complexity	385
VII The Density Matrix Representation	385

F	Two-Level Systems	389
I	Introduction to the Problem	389
I.1	Relation to Spin-1/2 Systems	390
II	Static Properties of Two-Level Systems	390
II.1	Eigenstates and Eigenvalues	390
II.2	Interpretation	391
II.3	Quantum Resonance	394
III	Dynamic Properties of Two-Level Systems	395
III.1	Time Evolution of the State Vector	395
III.2	The Rabi Formula	395
G	The Spin 1/2 System	399
I	Experimental Demonstration of Angular Momentum Quantization	399
II	Theoretical Description	401
II.1	The Spin Space	401
III	Evolution of a Spin 1/2 Particle in a Homogeneous Magnetic Field	402
IV	Spin 1/2 Particle in a Rotating Magnetic Field	404
IV.1	Classical Treatment	404
IV.2	Quantum Mechanical Treatment	406
IV.3	Rabi's Formula	407
H	Literature	409
I	Foundations of Superconductivity	409
I.1	Introduction to Superconductivity	409
I.2	Early Work on Superconductivity and Superfluidity	410
I.3	History of Superconductivity	410
I.4	Weak Superconductivity, Josephson Effect, Flux Structures	410
II	Applications of Superconductivity	411
II.1	Electronics, Sensors, Microwave Devices	411
II.2	Power Applications, Magnets, Transportation	412
II.3	Superconducting Materials	412
I	SI-Einheiten	413
I	Geschichte des SI Systems	413
II	Die SI Basiseinheiten	415
III	Einige von den SI Einheiten abgeleitete Einheiten	416
IV	Vorsätze	418
V	Abgeleitete Einheiten und Umrechnungsfaktoren	419

J Physikalische Konstanten**425**

List of Figures

1.1	Meissner-Effect	19
1.2	Current transport and decay of a supercurrent in the Fermi sphere picture	20
1.3	Stationary Quantum States	24
1.4	Flux Quantization in Superconductors	25
1.5	Flux Quantization in a Superconducting Cylinder	27
1.6	Experiment by Doll and Naebauer	29
1.7	Experimental Proof of Flux Quantization	29
1.8	Rotating superconducting cylinder	31
1.9	The Josephson Effect in weakly coupled superconductors	32
1.10	Variation of n_s^* and γ across a Josephson junction	35
1.11	Schematic View of a Josephson Junction	36
1.12	Josephson Tunneling	39
2.1	Lumped Josephson Junction	45
2.2	Coupling Energy and Josephson Current	46
2.3	The Tilted Washboard Potential	48
2.4	Extended Josephson Junction	51
2.5	Magnetic Field Dependence of the Maximum Josephson Current	55
2.6	Josephson Current Distribution in a Small Josephson Junction for Various Applied Magnetic Fields	56
2.7	Spatial Interference of Macroscopic Wave Funktionen	57
2.8	The Josephson Vortex	57
2.9	Gaussian Shaped Josephson Junction	59
2.10	Comparison between Measurement of Maximum Josephson Current and Optical Diffraction Experiment	60
2.11	Supercurrent Auto-correlation Function	61
2.12	Magnetic Field Dependence of the Maximum Josephson Current of a YBCO-GBJ	63

2.13	Motion of Josephson Vortices	66
2.14	Magnetic Flux and Current Density Distribution for a Josephson Vortex	70
2.15	Classification of Junction Types: Overlap, Inline and Grain Boundary Junction	74
2.16	Geometry of the Asymmetric Inline Junction	77
2.17	Geometry of Mixed Overlap and Inline Junctions	78
2.18	The Josephson Current Distribution of a Long Inline Junction	80
2.19	The Maximum Josephson Current as a Function of the Junction Length	81
2.20	Magnetic Field Dependence of the Maximum Josephson Current and the Josephson Current Density Distribution in an Overlap Junction	83
2.21	The Maximum Josephson Current as a Function of the Applied Field for Overlap and Inline Junctions	84
3.1	Current-Voltage Characteristic of a Josephson tunnel junction	91
3.2	Equivalent circuit for a Josephson junction including the normal, displacement and fluctuation current	92
3.3	Equivalent circuit of the Resistively Shunted Junction Model	97
3.4	The Motion of a Particle in the Tilt Washboard Potential	98
3.5	Pendulum analogue of a Josephson junction	99
3.6	The IVCs for Underdamped and Overdamped Josephson Junctions	101
3.7	The time variation of the junction voltage and the Josephson current	103
3.8	The RSJ model current-voltage characteristics	105
3.9	The RCSJ Model IVC at Intermediate Damping	107
3.10	The RCJ Model Circuit for an Applied dc and ac Voltage Source	108
3.11	Overdamped Josephson Junction driven by a dc and ac Voltage Source	110
3.12	Overdamped Josephson junction driven by a dc and ac Current Source	111
3.13	Shapiro steps for under- and overdamped Josephson junction	112
3.14	Photon assisted tunneling	113
3.15	Photon assisted tunneling in SIS Josephson junction	113
3.16	Thermally Activated Phase Slippage	116
3.17	Temperature Dependence of the Thermally Activated Junction Resistance	119
3.18	RSJ Model Current-Voltage Characteristics Including Thermally Activated Phase Slippage	120
3.19	Variation of the Josephson Coupling Energy and the Charging Energy with the Junction Area	124
3.20	Energy diagrams of an isolated Josephson junction	127
3.21	The Coulomb Blockade	128

3.22	The Phase Blockade	129
3.23	The Cooper pair box	131
3.24	Double well potential for the generation of phase superposition states	132
3.25	Macroscopic Quantum Tunneling	134
3.26	Macroscopic Quantum Tunneling at Large Damping	138
3.27	Mechanical analogue for phase dynamics of a long Josephson junction	141
3.28	The Current Voltage Characteristic of an Underdamped Long Josephson Junction	145
3.29	Zero field steps in IVCs of an annular Josephson junction	147
4.1	The dc-SQUID	160
4.2	Maximum Supercurrent versus Applied Magnetic Flux for a dc-SQUID at Weak Screening	162
4.3	Total Flux versus Applied Magnetic Flux for a dc SQUID at $\beta_L > 1$	163
4.4	Current-voltage Characteristics of a dc-SQUID at Negligible Screening	165
4.5	The pendulum analogue of a dc SQUID	167
4.6	Principle of Operation of a dc-SQUID	169
4.7	Energy Resolution of dc-SQUIDs	172
4.8	The Practical dc-SQUID	173
4.9	Geometries for thin film SQUID washers	174
4.10	Flux focusing effect in a $\text{YBa}_2\text{Cu}_3\text{O}_{7-\delta}$ washer	175
4.11	The Washer dc-SQUID	176
4.12	The Flux Modulation Scheme for a dc-SQUID	177
4.13	The Modulation and Feedback Circuit of a dc-SQUID	178
4.14	The rf-SQUID	180
4.15	Total flux versus applied flux for a rf-SQUID	182
4.16	Operation of rf-SQUIDs	183
4.17	Tank voltage versus rf-current for a rf-SQUID	184
4.18	High T_c rf-SQUID	187
4.19	The double relaxation oscillation SQUID (DROS)	188
4.20	The Superconducting Quantum Interference Filter (SQIF)	190
4.21	Input Antenna for SQUIDs	191
4.22	Various types of thin film SQUID magnetometers	193
4.23	Magnetic noise signals	194
4.24	Magnetically shielded room	195
4.25	Various gradiometers configurations	196

4.26	Miniature SQUID Susceptometer	197
4.27	SQUID Radio-frequency Amplifier	198
4.28	Multichannel SQUID Systems	201
4.29	Magnetocardiography	203
4.30	Magnetic field distribution during R peak	204
4.31	SQUID based nondestructive evaluation	205
4.32	Scanning SQUID microscopy	207
4.33	Scanning SQUID microscopy images	208
4.34	Gravity wave antenna	209
4.35	Gravity gradiometer	210
5.1	Cryotron	217
5.2	Josephson Cryotron	218
5.3	Device performance of Josephson devices	220
5.4	Principle of operation of a Josephson switching device	222
5.5	Output current of a Josephson switching device	224
5.6	Threshold characteristics for a magnetically and directly coupled gate	229
5.7	Three-junction interferometer gate	230
5.8	Current injection device	230
5.9	Josephson Atto Weber Switch (JAWS)	231
5.10	Direct coupled logic (DCL) gate	231
5.11	Resistor coupled logic (RCL) gate	232
5.12	4 junction logic (4JL) gate	232
5.13	Non-destructive readout memory cell	234
5.14	Destructive read-out memory cell	235
5.15	4 bit Josephson microprocessor	237
5.16	Josephson microprocessor	238
5.17	Comparison of latching and non-latching Josephson logic	240
5.18	Generation of SFQ Pulses	242
5.19	dc to SFQ Converter	243
5.20	Basic Elements of RSFQ Circuits	244
5.21	RSFQ memory cell	245
5.22	RSFQ logic	246
5.23	RSFQ OR and AND Gate	247

5.24	RSFQ NOT Gate	248
5.25	RSFQ Shift Register	249
5.26	RSFQ Microprocessor	253
5.27	RSFQ roadmap	254
5.28	Principle of operation of an analog-to-digital converter	256
5.29	Analog-to-Digital Conversion	257
5.30	Semiconductor and Superconductor Comparators	262
5.31	Incremental Quantizer	263
5.32	Flash-type ADC	265
5.33	Counting-type ADC	266
6.1	Weston cell	271
6.2	The metrological triangle for the electrical units	273
6.3	IVC of an underdamped Josephson junction under microwave irradiation	275
6.4	International voltage comparison between 1920 and 2000	276
6.5	One-Volt Josephson junction array	277
6.6	Josephson series array embedded into microwave stripline	278
6.7	Microwave design of Josephson voltage standards	279
6.8	Adjustment of Shapiro steps for a series array Josephson voltage standard	281
6.9	IVC of overdamped Josephson junction with microwave irradiation	282
6.10	Programmable Josephson voltage standard	283
7.1	Block diagram of a heterodyne receiver	288
7.2	Ideal mixer as a switch	288
7.3	Current response of a heterodyne mixer	289
7.4	IVCs and IF output power of SIS mixer	290
7.5	Optimum noise temperature of a SIS quasiparticle mixer	293
7.6	Measured DSB noise temperature of a SIS quasiparticle mixers	294
7.7	High frequency coupling schemes for SIS mixers	295
7.8	Principle of thermal detectors	301
7.9	Operation principle of superconducting transition edge bolometer	302
7.10	Sketch of a HTS bolometer	305
7.11	Specific detectivity of various bolometers	305
7.12	Relaxation processes in a superconductor after energy absorption	307
7.13	Antenna-coupled microbolometer	308

7.14	Schematic illustration of the hot electron bolometer mixer	309
7.15	Hot electron bolometer mixers with different antenna structures	311
7.16	Transition-edge sensors	315
7.17	Transition-edge sensors	317
7.18	Functional principle of a superconducting tunnel junction detector	319
7.19	Circuit diagram of a superconducting tunnel junction detector	319
7.20	Energy resolving power of STJDs	321
7.21	Quasiparticle tunneling in SIS junctions	323
7.22	Quasiparticle trapping in STJDs	326
7.23	STJDs employing lateral quasiparticle trapping	326
7.24	Superconducting tunnel junction x-ray detector	327
8.1	Equivalent circuit for the two-fluid model	332
8.2	Characteristic frequency regimes for a superconductor	332
8.3	Surface resistance of Nb and Cu	335
9.1	Konrad Zuse 1945	341
9.2	Representation of a Qubit State as a Vector on the Bloch Sphere	342
9.3	Operational Scheme of a Quantum Computer	344
9.4	Quantum Computing: What's it good for?	345
9.5	Shor, Feynman, Bennett and Deutsch	346
9.6	Qubit Realization by Quantum Mechanical Two level System	349
9.7	Use of Superconductors for Qubits	352
9.8	Superconducting Island with Leads	354
E.1	The Bloch Sphere S^2	370
E.2	The Spin-1/2 System	371
E.3	Entanglement – an artist's view.	373
E.4	Classical Single-Bit Gate	377
E.5	Quantum NOT Gate	378
E.6	Classical Two Bit Gate	380
E.7	Reversible and Irreversible Logic	380
E.8	Reversible Classical Logic	381
E.9	Reversible XOR (CNOT) and SWAP Gate	382
E.10	The Controlled U Gate	382

E.11	Density Matrix for Pure Single Qubit States	386
E.12	Density Matrix for a Coherent Superposition of Single Qubit States	387
F.1	Energy Levels of a Two-Level System	392
F.2	The Benzene Molecule	394
F.3	Graphical Representation of the Rabi Formula	396
G.1	The Larmor Precession	400
G.2	The Rotating Reference Frame	404
G.3	The Effective Magnetic Field in the Rotating Reference Frame	405
G.4	Rabi's Formula for a Spin 1/2 System	408

List of Tables

5.1	Switching delay and power dissipation for various types of logic gates.	233
5.2	Josephson 4 kbit RAM characteristics (organization: 4096 word × 1 bit, NEC).	236
5.3	Performance of various logic gates	237
5.4	Possible applications of superconductor digital circuits (source: SCENET 2001).	251
5.5	Performance of various RSFQ based circuits.	252
7.1	Characteristic materials properties of some superconductors	325
8.1	Important high-frequency characteristic of superconducting and normal conducting . . .	334
E.1	Successive measurements on a two-qubit state showing the results A and B with the corresponding probabilities $P(A)$ and $P(B)$ and the remaining state after the measurement. . . .	373

Chapter E

Foundations of Quantum Bits and Gates

I What is a quantum bit ?

Classical computing is based on classical (c-) bits that are usually represented by “0” and “1”. Mathematically we have to deal with a binary variable

$$x \in \{0,1\} \tag{I.1}$$

with the property $x^2 = x$. Physically, these two states can be represented in different ways as for example by “charge on a capacitor” and “no charge on a capacitor”, by “magnetization direction to the left” and “magnetization direction to the right” or by “hole in the punch card” and “no hole in the punch card”. The bits are manipulated by classical single (e.g. NOT) or multiple bit gates (e.g. AND, NAND, OR, NOR, ...) as discussed in more detail in section IV. For example, a two bit gate is transferring the two bits x and y with $(x,y) \in \{0,1\}$ to $f(x,y)$ with $f(x,y) \in \{0,1\}$.

I.1 Single-Qubit Systems

Whereas classical computers operate with *classical (c-) bits*, quantum computers operate with *quantum (qu-) bits* usually denoted as *qubits*. Physically, a qubit can be represented by every two level quantum system. With the basis states of a two level quantum system (e.g. a spin-1/2 system)

$$|\phi_1\rangle = |0\rangle = |\uparrow\rangle = \begin{pmatrix} 1 \\ 0 \end{pmatrix} \tag{I.2}$$

$$|\phi_2\rangle = |1\rangle = |\downarrow\rangle = \begin{pmatrix} 0 \\ 1 \end{pmatrix} \tag{I.3}$$

we can define a one qubit state in the following way:

A qubit $|\Psi\rangle$ is the superposition of two computational basis states

$$|\Psi(t)\rangle = a(t)|0\rangle + b(t)|1\rangle = \begin{pmatrix} a(t) \\ b(t) \end{pmatrix}, \tag{I.4}$$

where $a(t)$ and $b(t)$ are complex amplitudes.

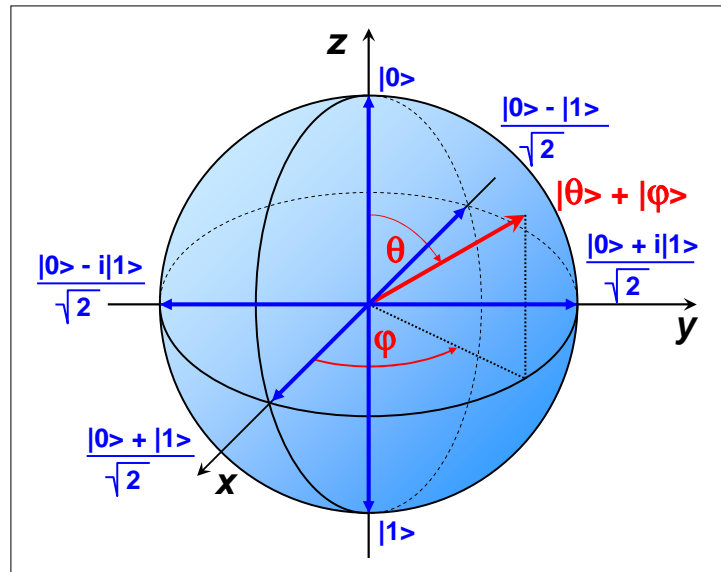


Figure E.1: Geometrical representation of a qubit state as a vector on the Bloch sphere S^2 .

It is important to note that a and b are continuous analogue variables. If we are measuring the quantum state of a qubit, we obtain the result $|0\rangle$ with probability $|a(t)|^2$ and the result $|1\rangle$ with probability $|b(t)|^2$. Since the total probability must be unity we have the normalization condition

$$\langle \Psi(t) | \Psi(t) \rangle = |a(t)|^2 + |b(t)|^2 = 1. \quad (\text{I.5})$$

We see that the qubit exists in a continuum of states. It is a superposition of two basis states and therefore can be represented as a unit vector in a two-dimensional Hilbert space \mathcal{H}_2 .

A general form of the one-qubit state satisfying (E.I.5) is given by

$$|\Psi(t)\rangle \equiv |\theta, \varphi\rangle = \cos \frac{\theta}{2} e^{-i\varphi/2} |0\rangle + \sin \frac{\theta}{2} e^{+i\varphi/2} |1\rangle = \begin{pmatrix} \cos \frac{\theta}{2} e^{-i\varphi/2} \\ \sin \frac{\theta}{2} e^{+i\varphi/2} \end{pmatrix}. \quad (\text{I.6})$$

The geometrical representation of the qubit state can hence be given by a point on the Bloch sphere S^2 as shown in Fig. E.1.

We immediately can write down some special case for the qubit state $|\theta, \varphi\rangle$:

$$|\theta, \varphi\rangle = |0, \varphi\rangle = |0\rangle \quad (\text{I.7})$$

$$|\theta, \varphi\rangle = |\pi, \varphi\rangle = |1\rangle \quad (\text{I.8})$$

$$|\theta, \varphi\rangle = \left| \frac{\pi}{2}, 0 \right\rangle = \frac{|0\rangle + |1\rangle}{\sqrt{2}} \quad (\text{I.9})$$

$$|\theta, \varphi\rangle = \left| \frac{\pi}{2}, \pi \right\rangle = \frac{|0\rangle - |1\rangle}{\sqrt{2}}. \quad (\text{I.10})$$

These states are also indicated in Fig. E.1.

Note that there is an infinite number of possible qubit states. However, any measurement on the qubit state results in a collapse of the state and a reduction of the state to one of its basis states. Information on

a and b is only obtained by performing measurements on an ensemble of identical qubits and a statistical analysis. This is a specific advantage of the use of quantum bits in quantum information processing: As long as the quantum system is not perturbed, i.e. as long as we do not perform any measurement, the state keeps all continuous variables for the description of the state. That is, the quantum system keep all possible options until the state is destroyed by a measuring process. This results in a massive quantum parallelism that can speed up computing processes.

I.2 The spin-1/2 system

Since spin systems have been widely studied and today's magnetic resonance techniques are capable to prepare a spin system in any state and let it evolve in time, it is quite common to adopt the language of spin-1/2 systems to describe the preparation and manipulation of qubits (see Fig. E.2). We also will often do so in the following. The spin state again can be considered as a vector on the Bloch sphere shown in Fig. E.1. The controlled evolution of the spin state corresponding to the motion of the end point of the vector on the Bloch sphere can be obtained by applying control fields B_z and B_x or resonant microwave pulses to the system as discussed in more detail in Appendix G.

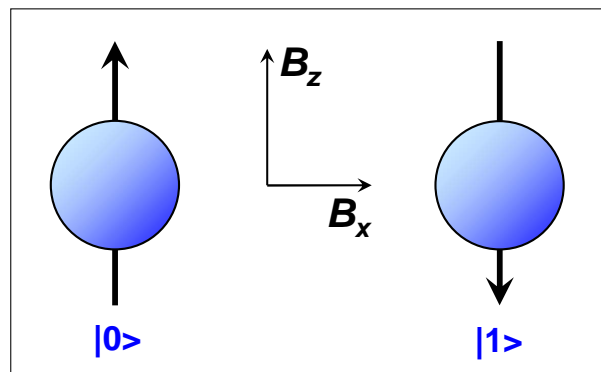


Figure E.2: The spin-1/2 system as an example for a two-level quantum system. The two basis state $|0\rangle$ and $|1\rangle$ correspond to the two possible spin orientations $|\uparrow\rangle$ and $|\downarrow\rangle$ with respect to the quantization axis given by the magnetic field B_z . A perpendicular magnetic field B_x results in the mixing of the two basis states.

I.3 Two-Qubit Systems

It is instructive to consider first two classical bits. The four possible states of a *classical two-bit system* are

$$|\phi_1\rangle = |00\rangle = \begin{pmatrix} 1 \\ 0 \\ 0 \\ 0 \end{pmatrix} \otimes \begin{pmatrix} 1 \\ 0 \end{pmatrix} = \begin{pmatrix} 1 \\ 0 \\ 0 \\ 0 \end{pmatrix} \quad (\text{I.11})$$

$$|\phi_2\rangle = |01\rangle = \begin{pmatrix} 1 \\ 0 \end{pmatrix} \otimes \begin{pmatrix} 0 \\ 1 \end{pmatrix} = \begin{pmatrix} 0 \\ 1 \\ 0 \\ 0 \end{pmatrix} \quad (\text{I.12})$$

$$|\phi_3\rangle = |10\rangle = \begin{pmatrix} 0 \\ 1 \end{pmatrix} \otimes \begin{pmatrix} 1 \\ 0 \end{pmatrix} = \begin{pmatrix} 0 \\ 0 \\ 1 \\ 0 \end{pmatrix} \quad (\text{I.13})$$

$$|\phi_4\rangle = |11\rangle = \begin{pmatrix} 0 \\ 1 \end{pmatrix} \otimes \begin{pmatrix} 0 \\ 1 \end{pmatrix} = \begin{pmatrix} 0 \\ 0 \\ 0 \\ 1 \end{pmatrix}. \quad (\text{I.14})$$

These four states are also the basis states of a *quantum two-bit system*, which is given by the superposition of these basis states

$$|\Psi(t)\rangle = c_{00}(t)|00\rangle + c_{01}(t)|01\rangle + c_{10}(t)|10\rangle + c_{11}(t)|11\rangle = \begin{pmatrix} c_{00} \\ c_{01} \\ c_{10} \\ c_{11} \end{pmatrix}. \quad (\text{I.15})$$

Similar as for the one-qubit system the four coefficients are complex, continuous and have to satisfy the normalization condition

$$\langle\Psi(t)|\Psi(t)\rangle = |c_{00}(t)|^2 + |c_{01}(t)|^2 + |c_{10}(t)|^2 + |c_{11}(t)|^2 = 1. \quad (\text{I.16})$$

We see that the two-qubit state is a superposition of four basis states and therefore can be represented as a unit vector in a four-dimensional Hilbert space \mathcal{H}_4 . Note that for a n -qubit state the number of coefficients increases to 2^n .

If we are performing measurements on a two-qubit state, we are perturbing the qubit state. The results A and B with the respective probabilities $P(A)$ and $P(B)$ of successive measurements of the first and second qubit are summarized in Table E.1.

We can now consider special states. If we assume for example that two of the four coefficients are zero, we obtain the following results for the measurement of the first (A) and the second qubit (B):

	$c_{00} = 0$	$c_{01} = 0$	$c_{10} = 0$	$c_{11} = 0$
$c_{00} = 0$	—	$A \equiv 1$	$B \equiv 1$	$B \equiv 1 - A$
$c_{01} = 0$	$A \equiv 1$	—	$B \equiv A$	$B \equiv 0$
$c_{10} = 0$	$B \equiv 1$	$B \equiv A$	—	$A \equiv 0$
$c_{11} = 0$	$B \equiv 1 - A$	$B \equiv 0$	$A \equiv 0$	—

	measurement of 1. qubit			measurement of 2. qubit	
A	$P(A)$	remaining state	B	$P(B)$	remaining state
0	$ c_{00} ^2 + c_{01} ^2$	$ \Psi'\rangle = \frac{c_{00} 00\rangle + c_{01} 01\rangle}{\sqrt{ c_{00} ^2 + c_{01} ^2}}$	0	$\frac{ c_{00} ^2}{ c_{00} ^2 + c_{01} ^2}$	$ 00\rangle$
			1	$\frac{ c_{01} ^2}{ c_{00} ^2 + c_{01} ^2}$	$ 01\rangle$
1	$ c_{10} ^2 + c_{11} ^2$	$ \Psi'\rangle = \frac{c_{10} 10\rangle + c_{11} 11\rangle}{\sqrt{ c_{10} ^2 + c_{11} ^2}}$	0	$\frac{ c_{10} ^2}{ c_{10} ^2 + c_{11} ^2}$	$ 10\rangle$
			1	$\frac{ c_{11} ^2}{ c_{10} ^2 + c_{11} ^2}$	$ 11\rangle$

Table E.1: Successive measurements on a two-qubit state showing the results A and B with the corresponding probabilities $P(A)$ and $P(B)$ and the remaining state after the measurement.

These results directly follow from Table E.1. If for example $c_{00} = c_{01} = 0$, the probability for the measurement result $A = 0$ is $P(A) = |c_{00}|^2 + |c_{01}|^2 = 0$. That is, that in a measurement we obtain always the result $A = 1$.

II Entanglement

Entanglement is a new kind of correlations between two subsystems of a quantum system, which does not exist in classical physics (or classical probability). The term is a translation of the German “*Verschränktheit*”, coined by **Erwin Schrödinger** in 1935.¹ Both notations reflect well the efforts of understanding such correlations in classical terms. However, from the point of view of quantum theory such correlations are rather straightforward and, in fact, ubiquitous.

Some correlations between quantum systems can be understood completely in classical terms: Suppose that two subsystems are prepared by two independent devices, whose operation may depend on the output of some classical random generator, which they both receive. In this case the source of the correlations is simply the classical random generator, and states produced in this way are called “classically correlated” or “separable”. The density operator of such a state is a convex combination of tensor products of density operators. All other states are called “entangled”. A simple example is a pure state, which happens not to be a product state. Since a pure state cannot be non-trivially decomposed into a convex combination of any other states, it also cannot be decomposed into products states, so it is not classically correlated. The fact that entangled states are not some bizarre but expendable feature of quantum mechanics but lead to observable effects, is shown most directly by Bell’s inequality. It is easy to show that these inequalities are satisfied by every classically correlated state, but they have been found violated in a series of now



¹E. Schrödinger, *Die gegenwärtige Situation in der Quantenmechanik*, *Die Naturwissenschaften* 23 807-812, 823-828, and 844-849 (1935).

famous experiments.² Hence, these experiments directly confirm the existence of entangled states.

In the theory of Quantum Information entanglement is viewed as a resource needed to perform otherwise impossible tasks of information processing or computation. There is a variety of tasks for which entanglement plays an important role and, correspondingly, a variety of quantitative measures of entanglement. For pure states most of these reduce to the von Neumann entropy of the restricted density operators. This is a quantitative version of a crucial special feature of quantum mechanics, namely that pure states of composite systems may be mixed when restricted to a subsystem, as measured by the von Neumann entropy.

For mixed states there are many quantitative notions of entanglement, some of which are provably different. Probably only a few such quantities will turn out to be useful as the theory develops. But it is much too early to say which the interesting ones are.

As an example we consider the situations where the results A and B of a measurement on a two-qubit state are correlated. This is for example the case for the following normalized two-qubit states, which we obtain for $c_{01} = c_{10} = 0$ and $c_{00} = c_{11} = 0$:

$$\frac{c_{00}(t)|00\rangle + c_{11}(t)|11\rangle}{\sqrt{|c_{00}|^2 + |c_{11}|^2}} \quad \text{or} \quad \frac{c_{01}(t)|01\rangle + c_{10}(t)|10\rangle}{\sqrt{|c_{01}|^2 + |c_{10}|^2}} . \quad (\text{II.17})$$

It is obvious that by measuring the quantum state of the first qubit of these states we also fix the quantum state of the second qubit. Such states are called *Bell states* or *Einstein-Podolsky-Rosen (EPR) pairs*.³ They represent *entangled states*.

In order to discuss entanglement a little bit more, we consider two quantum systems (such as two photon or two spins). If these two systems are not coupled, the wavefunction of the total systems is just given by the product of the two wavefunctions of the subsystems:

$$|0\rangle \cdot |1\rangle = |10\rangle \quad \text{or} \quad |1\rangle \cdot |0\rangle = |01\rangle . \quad (\text{II.18})$$

If there is a finite interaction between the subsystems, we obtain a coupling which is causing linear combinations of the wavefunction in (E.II.18). A well known example is

$$|\Psi\rangle = \frac{1}{\sqrt{2}} (|01\rangle - |10\rangle) , \quad (\text{II.19})$$

which corresponds to a spin singlet state for a spin system. Such linear combination of the product states is called *entanglement*. The EPR pairs discussed above represent entangled states. An important mathematical property of entangled states is the fact that they cannot be expressed as a product of the basis states. The important physical property of entangled states is the fact that the measurement of the one-qubit state is fixing the measurement result of the other. We will discuss in section III how we can produce entangled states by one- and two-qubit operations.

²A. Aspect, P. Grangier, G. Roger, *Experimental tests of realistic local theories via Bell's Theorem*, Phys. Rev. Lett. **47**, 460-463 (1981); see also Phys. Rev. Lett. **49**, 91-94 (1982); Phys. Rev. Lett. **49**, 1804-1807 (1982).

³A. Einstein, B. Podolsky, N. Rosen, *Can quantum mechanical description of physical reality be complete?*, Phys. Rev. **47** (1935).

III Qubit Operations

III.1 Unitarity

If we discuss possible manipulations of the qubit state we have to take into account the normalization condition (E.I.16). That is, during the time evolution of the qubit states we have to satisfy the normalization of the state. With the Schrödinger equation

$$i\hbar \frac{\partial}{\partial t} |\Psi\rangle = \mathcal{H} |\Psi\rangle \quad (\text{III.20})$$

the time evolution of the state can be expressed as

$$|\Psi(t)\rangle = \exp\left(-\frac{i}{\hbar} \mathcal{H} t\right) |\Psi(0)\rangle = \mathcal{U}(t) |\Psi(0)\rangle . \quad (\text{III.21})$$

Since we have to preserve normalization, we obtain

$$\langle \Psi(t) | \Psi(t) \rangle = \langle \Psi(0) | \mathcal{U}^\dagger(t) \mathcal{U}(t) | \Psi(0) \rangle = 1 . \quad (\text{III.22})$$

That is, we obtain the unitary condition

$$\mathcal{U}^\dagger(t) \mathcal{U}(t) = 1 \quad \rightarrow \quad \mathcal{U}^\dagger = \mathcal{U}^{-1} . \quad (\text{III.23})$$

We see that qubit operation in general have to be achieved with $n \times n$ unitary matrices with unit determinant. These matrices are forming the $SU(n)$ group. For a single-qubit we have to deal with the 2×2 matrices of the $SU(2)$ group.⁴

III.2 Single Qubit Operations

We use the spin-1/2 model system to discuss single-qubit operations. With the control fields B_z and B_x , which may be time dependent, the qubit Hamiltonian can be written in the spin-1/2 notation as

$$\mathcal{H} = -\mathcal{H}_z \mathbf{Z} - \mathcal{H}_x \mathbf{X} = -\frac{\hbar}{2} \gamma B_z \mathbf{Z} - \frac{\hbar}{2} \gamma B_x \mathbf{X} , \quad (\text{III.24})$$

where γ is the gyromagnetic ratio and the Pauli matrices in the space states $|\uparrow\rangle$ and $|\downarrow\rangle$ are given by

$$\vec{\sigma} = \{\mathbf{X}, \mathbf{Y}, \mathbf{Z}\} = \left\{ \begin{pmatrix} 0 & 1 \\ 1 & 0 \end{pmatrix}, \begin{pmatrix} 0 & -i \\ i & 0 \end{pmatrix}, \begin{pmatrix} 1 & 0 \\ 0 & -1 \end{pmatrix} \right\} . \quad (\text{III.25})$$

It is evident that the field B_z results in an energy splitting of the basis states $|\uparrow\rangle$ and $|\downarrow\rangle$ proportional to the applied magnetic field but does not mix these states. The magnetic field B_x in contrast results in a mixing of the basis state

A single-qubit operation can be performed, for example, by turning on the control field $B_x(t)$ for a time interval τ . As a result of this operation the quantum state evolves according to the unitary transformation

$$\mathcal{U}_x(\theta) = \exp\left(\frac{i\gamma B_x \tau}{2} \mathbf{X}\right) = \begin{pmatrix} \cos \frac{\theta}{2} & i \sin \frac{\theta}{2} \\ i \sin \frac{\theta}{2} & \cos \frac{\theta}{2} \end{pmatrix} = \cos \frac{\theta}{2} \mathbf{1} + i \sin \frac{\theta}{2} \mathbf{X} , \quad (\text{III.26})$$

⁴Note that unitarity is the Hilbert space equivalent of rotation matrix orthogonality (isomorphism $SU(2) \leftrightarrow SO(3)$).

where $\theta \equiv \gamma B_x \tau = \omega_x \tau$. For example, by proper choice of the time span τ we can achieve $\theta = \pi$ or $\theta = \pi/2$. This produces a spin flip (NOT operation) or an equal weight superposition of the spin states, respectively.

Switching on $B_z(t)$ for a time interval τ produces another basic single bit operation, namely a phase shift between $|\uparrow\rangle$ and $|\downarrow\rangle$. The unitary operation reads as

$$\mathcal{U}_z(\varphi) = \exp\left(\frac{i\gamma B_z \tau}{2} \mathbf{Z}\right) = \begin{pmatrix} e^{i\varphi/2} & 0 \\ 0 & e^{-i\varphi/2} \end{pmatrix}, \quad (\text{III.27})$$

where $\varphi \equiv \gamma B_z \tau = \omega_z \tau$. Note that with a sequence of these x - and z -rotations any unitary transformation of the qubit state can be achieved, that is, every position on the Bloch sphere can be accessed. There is no need to turn on B_y .

III.3 Two Qubit Operations

A two-qubit operation on two qubits i and j is induced by switching on a coupling $J^{ij}(t)$ for a time interval τ . According to (9.2.3) the coupling term can be expressed as

$$\mathcal{H}(t) = \sum_{i \neq j} J_{\alpha\beta}^{ij}(t) \vec{\sigma}_\alpha^i \vec{\sigma}_\beta^j, \quad (\text{III.28})$$

where the summation over the state (e.g. spin) indices α, β is implied. As an example we discuss the **XY** coupling of two spins:⁵

$$\mathcal{H}(t) = J^{ij}(t) \vec{\sigma}_\alpha^i \vec{\sigma}_\beta^j = J^{ij}(\mathbf{XX} + \mathbf{YY}) = 2J^{ij} \begin{pmatrix} 0 & 0 & 0 & 0 \\ 0 & 0 & 1 & 0 \\ 0 & 1 & 0 & 0 \\ 0 & 0 & 0 & 0 \end{pmatrix}. \quad (\text{III.29})$$

In the basis $|\uparrow\uparrow\rangle, |\uparrow\downarrow\rangle, |\downarrow\uparrow\rangle, |\downarrow\downarrow\rangle$ the result is described by the unitary operator

$$\mathcal{U}^{ij}(\gamma) = \exp\left(\frac{i2J^{ij}\tau}{\hbar}(\mathbf{XX} + \mathbf{YY})\right) = \begin{pmatrix} 1 & 0 & 0 & 0 \\ 0 & \cos \delta & i \sin \delta & 0 \\ 0 & i \sin \delta & \cos \delta & 0 \\ 0 & 0 & 0 & 1 \end{pmatrix}, \quad (\text{III.30})$$

where $\delta = 2J^{ij}\tau/\hbar = 2\omega_{ij}\tau$. For $\delta = \pi/2$ the operation leads to a swap (exchange) of the states $|\uparrow\downarrow\rangle$ ($|10\rangle$) and $|\downarrow\uparrow\rangle$ ($|01\rangle$) and an additional multiplication by i . In contrast, for $\delta = \pi/4$ the operation

⁵Note that for a **YY** coupling we obtain

$$\mathcal{H}(t) = J^{ij}\mathbf{YY} = J^{ij} \begin{pmatrix} 0 & 0 & 0 & -1 \\ 0 & 0 & 1 & 0 \\ 0 & 1 & 0 & 0 \\ -1 & 0 & 0 & 0 \end{pmatrix}$$

and for a **ZZ** coupling

$$\mathcal{H}(t) = J^{ij}\mathbf{ZZ} = J^{ij} \begin{pmatrix} 1 & 0 & 0 & 0 \\ 0 & -1 & 0 & 0 \\ 0 & 0 & -1 & 0 \\ 0 & 0 & 0 & 1 \end{pmatrix}.$$

transforms the state $|\uparrow\downarrow\rangle$ into an entangled state $\frac{1}{\sqrt{2}}(|\uparrow\downarrow\rangle + i|\downarrow\uparrow\rangle)$ (this is equivalent to the \sqrt{i} SWAP gate, see IV).

It is evident that the qubit operations must be realized by unitary operators ($UU^\dagger = U^\dagger U = 1$). First, the normalization condition must be valid for the qubit state after the operation. Therefore, the absolute value of the determinant of the matrix must be unity. In this way we rotate the qubit vector on the Bloch sphere without changing its length. Second, the operation must be reversible, that is the matrix must be invertible. Note that classical computation is not reversible since heat is dissipated during the operations thereby making the computation thermodynamically irreversible. This is not possible for quantum computers, since the superposition of the quantum states must be maintained during the whole computational process. If heat would be dissipated in an uncontrolled way, the coherence of the quantum state would be lost.

We note that so far we only considered the sudden switching of $B_{z,x}^i(t)$ or $J^{ij}(t)$. This is called a **non-adiabatic process**. However, one can also use other techniques to implement single or two qubit operations. For example, one can induce Rabi oscillations between different states of a qubit or a qubit pair by ac resonance signals. Furthermore, one can perform adiabatic manipulations of the qubits Hamiltonian to exchange different eigenstates with the occupations remaining unchanged.

IV Quantum Logic Gates

In the previous subsection we have shown how we can use unitary operators to realize manipulations of one- and two-qubit states. The details of the physical realization of an unitary operation such as the application of a magnetic field pulse or the way how one couples two qubits of course depend on the specific model system that is considered (e.g. spin, superconducting phase qubit, etc.). Quantum information theory, on the other hand, discusses quantum computation in a treatment that is independent of the physical system used to implement quantum computation. Here, the quantum algorithms are built out of standard single- and two-qubit gates. In the following we will discuss a several of them. In order to implement a quantum algorithm on a physical system we have to know how to express these standard gates in terms of the unitary operations specific to a physical system.

IV.1 Single-Bit Gates

We first consider **classical single-bit gates**. As shown in Fig. E.4, a single-bit gate acting on the binary variable x is transferring this variable to the $f(x)$, which is again a binary variable:

$$x \rightarrow f(x) \quad \text{with} \quad x \in \{0,1\} \quad \text{and} \quad f(x) \in \{0,1\} . \quad (\text{IV.31})$$

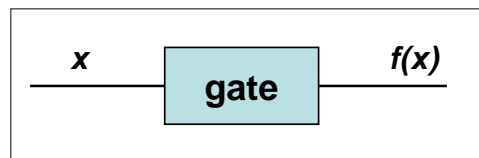


Figure E.4: The classical-single bit gate.

Prominent examples for the classical single-bit gate are the NOT, IDENTITY or RESET gates:

$$\text{NOT} \quad f(x) = \text{NOT}(x) = 1 - x \quad (\text{IV.32})$$

$$\text{IDENTITY} \quad f(x) = \text{IDENTITY}(x) = x \quad (\text{IV.33})$$

$$\text{RESET} \quad f(x) = \text{RESET}(x) = 0 . \quad (\text{IV.34})$$

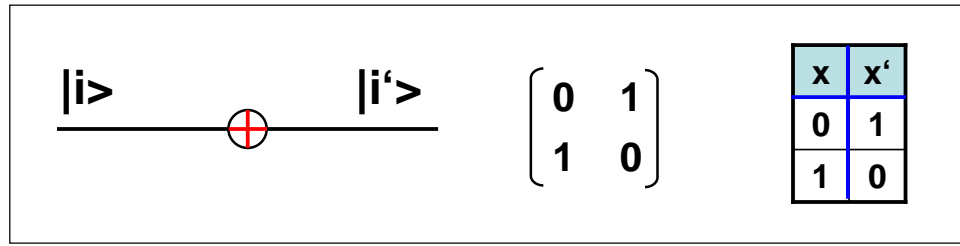


Figure E.5: The quantum NOT gate with the corresponding unitary matrix and the truth table.

Discussing the *quantum realization of single-bit gates* we have to use the unitary transformations discussed in the previous subsection:

Rotations about the x -axis are obtained by

$$\mathcal{U}_x(\theta) = \begin{pmatrix} \cos \frac{\theta}{2} & i \sin \frac{\theta}{2} \\ i \sin \frac{\theta}{2} & \cos \frac{\theta}{2} \end{pmatrix} = \cos \frac{\theta}{2} \mathbf{1} + i \sin \frac{\theta}{2} \mathbf{X}. \quad (\text{IV.35})$$

We see that a rotation about the x -axis by an arbitrary angle θ interpolates between the classical gates IDENTITY and NOT. The quantum NOT gate (see Fig. E.5)

$$\text{NOT} = \begin{pmatrix} 0 & 1 \\ 1 & 0 \end{pmatrix} = \mathbf{X} = e^{-i\frac{\pi}{2}} \mathcal{U}_x(\pi) \quad (\text{IV.36})$$

permutes the basis vectors $|0\rangle \rightarrow |1\rangle$ and $|1\rangle \rightarrow |0\rangle$. We see that it can be realized (up to an unimportant overall phase factor) by the unitary operation (x -rotation) of (E.III.26) with a properly chosen time interval τ resulting in $\theta \equiv B_x \tau / \hbar = \pi$: $\mathcal{U}_x(\theta = \pi) = i \cdot \text{NOT}$.

In contrast to classical computation in quantum logic there is a logic gate called $\sqrt{\text{NOT}}$, that when applied twice produces the NOT gate:

$$\sqrt{\text{NOT}} = \frac{1}{\sqrt{2i}} \begin{pmatrix} 0 & i \\ i & 0 \end{pmatrix} = \frac{1}{2} \begin{pmatrix} 1+i & -1+i \\ -1+i & 1+i \end{pmatrix} = \sqrt{\mathbf{X}} = e^{-i\frac{\pi}{4}} \mathcal{U}_x\left(\frac{\pi}{2}\right) \quad (\text{IV.37})$$

This gate is also obtained by the unitary operation (x -rotation) of (E.III.26) with $\theta \equiv B_x \tau / \hbar = \pi/2$, more precisely $\mathcal{U}_x(\theta = \pi/2) = \sqrt{i} \cdot \sqrt{\text{NOT}}$.

Rotations of a one-qubit state about the z -axis are obtained by the unitary operation (compare (E.III.27))

$$\mathcal{U}_z(\varphi) = \begin{pmatrix} e^{i\varphi/2} & 0 \\ 0 & e^{-i\varphi/2} \end{pmatrix} = e^{i\frac{\varphi}{2}} \begin{pmatrix} 1 & 0 \\ 0 & e^{-i\varphi} \end{pmatrix}. \quad (\text{IV.38})$$

The action on a qubit results in a relative phase shift φ

$$\mathcal{U}_z(\varphi)|0\rangle = |0\rangle \quad (\text{IV.39})$$

$$\mathcal{U}_z(\varphi)|1\rangle = e^{-i\varphi}|1\rangle. \quad (\text{IV.40})$$

Special cases are the **Z** gate

$$\mathbf{Z} = e^{-i\frac{\pi}{2}} \mathcal{U}_z(\pi) = \begin{pmatrix} 1 & 0 \\ 0 & -1 \end{pmatrix}, \quad (\text{IV.41})$$

the **S** gate

$$\mathbf{S} = \sqrt{\mathbf{Z}} = \begin{pmatrix} 1 & 0 \\ 0 & i \end{pmatrix} = \begin{pmatrix} 1 & 0 \\ 0 & e^{i\frac{\pi}{2}} \end{pmatrix}, \quad (\text{IV.42})$$

and the **T** gate

$$\mathbf{T} = \sqrt{\mathbf{S}} = \begin{pmatrix} 1 & 0 \\ 0 & e^{i\frac{\pi}{4}} \end{pmatrix}. \quad (\text{IV.43})$$

The **Hadamard gate** is another important, essentially quantum mechanical, single bit gate defined as

$$\mathbf{H} \equiv \frac{1}{\sqrt{2}} \begin{pmatrix} 1 & 1 \\ 1 & -1 \end{pmatrix} = \frac{\mathbf{X} + \mathbf{Z}}{\sqrt{2}}. \quad (\text{IV.44})$$

This gate, which is composed of a y - and z -rotation transforms the basis vectors into superpositions:

$$\mathbf{H}|0\rangle = \frac{1}{\sqrt{2}} (|0\rangle + |1\rangle) = |+\rangle \quad \text{and} \quad \mathbf{H}|1\rangle = \frac{1}{\sqrt{2}} (|0\rangle - |1\rangle) = |-\rangle. \quad (\text{IV.45})$$

The Hadamard gate is used to prepare a specific initial state. When applied to the ground state $|00\dots 0\rangle$, it provides an equally weighted superposition of all basis states:

$$\mathbf{H} \otimes \dots \otimes \mathbf{H} |0\dots 0\rangle = \frac{1}{2^{N/2}} \sum_{a_1 \dots a_N = 0,1} |a_1 \dots a_N\rangle. \quad (\text{IV.46})$$

The terms in the sum can be viewed as binary representations of all integers from 0 up to $2^N - 1$. Therefore, the state (E.IV.46) represents a superposition of all these integers. When this state is used as an input state for a quantum algorithm, it represents 2^N classical inputs. Due to the linearity of the quantum time evolution these inputs are processed simultaneously and the output is a superposition of 2^N classical results. This massive **quantum parallelism** is a key property of quantum computation and is responsible for the exponential speedup of certain quantum algorithms.

IV.2 Two Bit Gates

We again first consider **classical two-bit gates**. As shown in Fig. E.6, a two-bit gate acting on the binary variable (x, y) is transferring this variable to $f(x, y)$, which is again a binary variable:

$$(x, y) \rightarrow f(x, y) \quad \text{with} \quad (x, y) \in \{0, 1\} \quad \text{and} \quad f(x, y) \in \{0, 1\}. \quad (\text{IV.47})$$

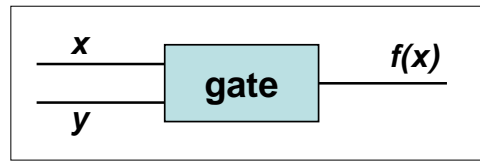


Figure E.6: The classical two-bit gate.

Prominent examples for classical two-bit gates are

$$f(x,y) = (x \text{ AND } y) = xy \tag{IV.48}$$

$$f(x,y) = (x \text{ NAND } y) = \text{NOT}(x \text{ AND } y) = 1 - xy \tag{IV.49}$$

$$f(x,y) = (x \text{ OR } y) = x + y - xy \tag{IV.50}$$

$$f(x,y) = (x \text{ NOR } y) = \text{NOT}(x \text{ OR } y) = 1 + xy - x - y \tag{IV.51}$$

$$f(x,y) = (x \text{ EQUIV } y) = \delta_{xy} \tag{IV.52}$$

$$f(x,y) = (x \text{ XOR } y) = x \oplus y = \text{NOT}(x \text{ EQUIV } y) = 1 - \delta_{xy} . \tag{IV.53}$$

The truth table of these operations is given by

(x,y)	AND	NAND	OR	NOR	EQUIV	XOR
0 0	0	1	0	1	1	0
0 1	0	1	1	0	0	1
1 0	0	1	1	0	0	1
1 1	1	0	1	0	1	0

It is evident from Fig. E.6 and the truth table that the two-bit gates discussed so far are *irreversible gates*. The difference between *reversible* and *irreversible* gates is shown in Fig. E.7. After the operation we can no longer reverse the operation to determine the input states. That is, information is lost what is resulting in an increase of entropy by $\Delta S = k_B \ln 2$ (Leo Szillard, 1929). It can further be shown that not all of the logical gates are required. Only a small *universal set of gates* is necessary to construct all other gates. It can be shown that the NAND gate is sufficient to produce all other gates.

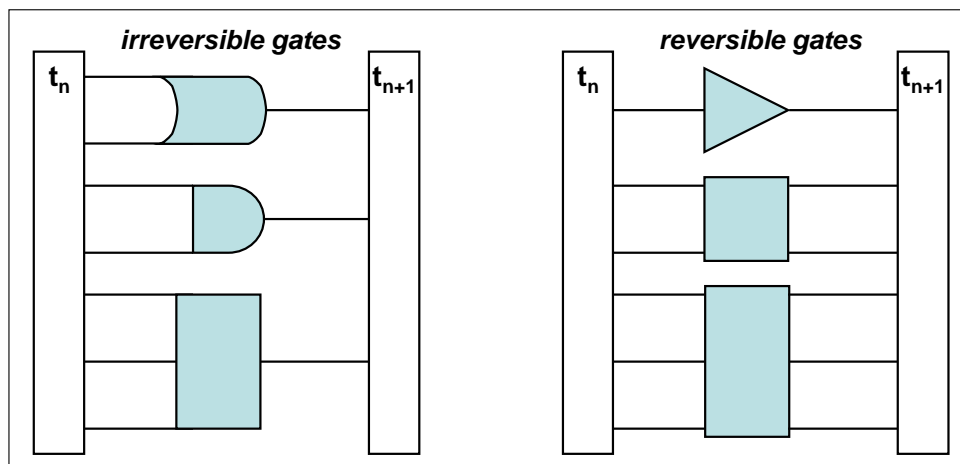


Figure E.7: Irreversible (left) and reversible (right) gates.

In the 1970ies a *reversible classical logic* has been established (Bennett, 1973). The structure of a classical reversible gate is shown in Fig. E.8. Reversibility is achieved by storage of the input bit x . A

typical example is the controlled NOT (CNOT) gate corresponding to a reversible exclusive OR (XOR) gate as shown in Fig. E.9a. The operation of the CNOT gate is defined as:

$$(x,y) \rightarrow \text{CNOT}(x,y) = (x, x \oplus y) = (x, 1 - \delta_{xy}) . \tag{IV.54}$$

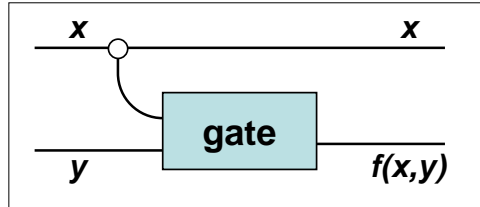


Figure E.8: Reversible classical logic gate.

A further important reversible gate is the SWAP gate that interchanges x and y (see Fig. E.9b):⁶

$$\begin{aligned} (x,y) &\rightarrow (x, x \oplus y) \\ (x,x \oplus y) &\rightarrow (x \oplus (x \oplus y), x \oplus y) = (y, x \oplus y) \\ (y,x \oplus y) &\rightarrow (y, (x \oplus y) \oplus y) = (y,x) . \end{aligned} \tag{IV.55}$$

We next have to discuss *two-bit quantum gates*. In the same way as for classical two-bit gates there exists a *universal set of two-qubit quantum gates* that is required to construct all other gates. It can be shown that the CNOT gate together with the one-qubit rotations $\mathbf{X}, \mathbf{Y}, \mathbf{Z}, \mathbf{S}, \mathbf{T}, \dots$ discussed above are sufficient to produce all other gates. That is, for the implementation of a quantum computer we only have to realize the CNOT gate and the single qubit rotations. With respect to two-bit quantum gates we therefore have to discuss mainly the CNOT gate.

Before describing the quantum CNOT gate we first introduce the more general controlled U (CU) gate shown in Fig. E.10:

$$\text{CU} |ij\rangle = \text{CU} |i\rangle \otimes |j\rangle = |i\rangle \otimes \{ \delta_{i0} |j\rangle + \delta_{i1} \mathcal{U} |j\rangle \} . \tag{IV.56}$$

⁶Proof that $x \oplus (x \oplus y) \equiv y$:

(x,y)	$x \oplus y$	$x \oplus (x \oplus y)$	y
0 0	0	0	0
0 1	1	1	1
1 0	1	0	0
1 1	0	0	1

Proof that $(x \oplus y) \oplus y \equiv x$:

(x,y)	$x \oplus y$	$(x \oplus y) \oplus y$	x
0 0	0	0	0
0 1	1	0	0
1 0	1	1	1
1 1	0	1	1

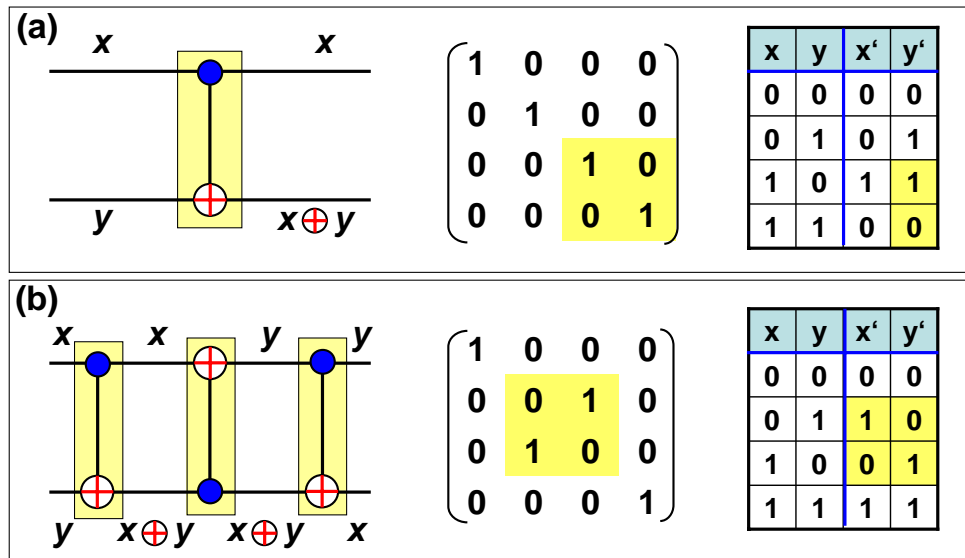


Figure E.9: The reversible XOR (CNOT) gate (a) and the SWAP gate (b) with the corresponding matrix and truth tables.

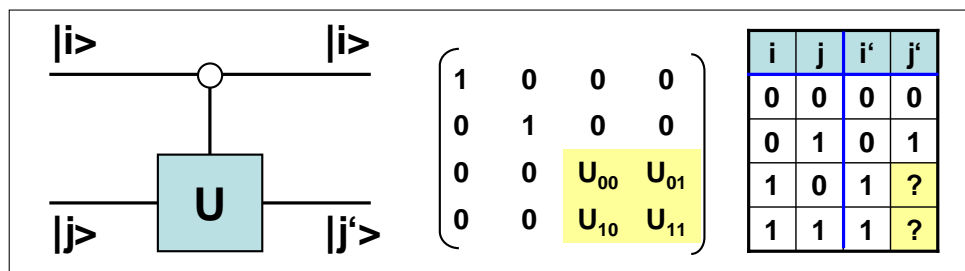


Figure E.10: The controlled U gate.

In a 4×4 matrix representations the CU gate can be expressed as

$$\mathcal{U} = \begin{pmatrix} 1 & 0 & 0 & 0 \\ 0 & 1 & 0 & 0 \\ 0 & 0 & \mathcal{U}_{00} & \mathcal{U}_{01} \\ 0 & 0 & \mathcal{U}_{10} & \mathcal{U}_{11} \end{pmatrix} = \begin{pmatrix} 1 & 0 \\ 0 & \mathcal{U} \end{pmatrix}. \tag{IV.57}$$

The controlled NOT gate represents a special case of the CU gate with \mathcal{U} being the quantum NOT or X gate.⁷ With (E.IV.36) we obtain

⁷The CNOT gate is therefore also called the CX gate.

Claim:

$$\text{CNOT} |ij\rangle = \text{CNOT} |i\rangle \otimes |j\rangle = |i\rangle \otimes \{\delta_{i0}|j\rangle + \delta_{i1}\text{NOT}|j\rangle\}.$$

Proof:

$$\begin{aligned} \text{CNOT} |i\rangle \otimes |j\rangle &= |i\rangle \otimes |1 - \delta_{ij}\rangle \\ &= |0\rangle \otimes \{\delta_{00}|j\rangle + \delta_{01}\text{NOT}|j\rangle\} = |0\rangle \otimes |j\rangle \quad \text{for } i = 0 \\ &= |1\rangle \otimes \{\delta_{10}|j\rangle + \delta_{11}\text{NOT}|j\rangle\} = |1\rangle \otimes \text{NOT}|j\rangle \quad \text{for } i = 1. \end{aligned}$$

$$\text{CNOT} = \begin{pmatrix} 1 & 0 & 0 & 0 \\ 0 & 1 & 0 & 0 \\ 0 & 0 & 0 & 1 \\ 0 & 0 & 1 & 0 \end{pmatrix} = \begin{pmatrix} 1 & 0 \\ 0 & \mathbf{X} \end{pmatrix}. \quad (\text{IV.58})$$

The CNOT gate flips the second qubits only if the first qubits is in the $|1\rangle$ state.

A further example is the *controlled phase gate*

$$C-\varphi = \begin{pmatrix} 1 & 0 & 0 & 0 \\ 0 & 1 & 0 & 0 \\ 0 & 0 & 0 & 0 \\ 0 & 0 & 0 & e^{-i\varphi} \end{pmatrix} = \begin{pmatrix} 1 & 0 \\ 0 & e^{-i\varphi} \mathcal{U}_z(\varphi) \end{pmatrix}, \quad (\text{IV.59})$$

which shifts the phase of state $|1\rangle$ of the second qubit when the first qubit is in the state $|1\rangle$.

As a further important two bit quantum gate we discuss the SWAP gate, which is produced by three CNOT gates in series:

$$\text{SWAP} = \text{CNOT}_{12} \cdot \text{CNOT}_{21} \cdot \text{CNOT}_{12} = \begin{pmatrix} 1 & 0 & 0 & 0 \\ 0 & 0 & 1 & 0 \\ 0 & 1 & 0 & 0 \\ 0 & 0 & 0 & 1 \end{pmatrix}. \quad (\text{IV.60})$$

and the $\sqrt{i\text{SWAP}}$ gate, “square root of the complex SWAP operation”

$$\sqrt{i\text{SWAP}} = \begin{pmatrix} 1 & 0 & 0 & 0 \\ 0 & \frac{1}{\sqrt{2}} & \frac{i}{\sqrt{2}} & 0 \\ 0 & \frac{i}{\sqrt{2}} & \frac{1}{\sqrt{2}} & 0 \\ 0 & 0 & 0 & 1 \end{pmatrix}. \quad (\text{IV.61})$$

The result of the SWAP operation is

$$\text{SWAP}|i, j\rangle = |j, i\rangle. \quad (\text{IV.62})$$

That is, the SWAP operation results in an exchange of the two input qubits $|i\rangle$ and $|j\rangle$. In contrast, the $\sqrt{i\text{SWAP}}$ operation transforms the state $|10\rangle$ into an entangled state $\frac{1}{\sqrt{2}}(|10\rangle + i|01\rangle)$.

The two-qubit gates can be realized by two-qubit operations as described in section III. We only consider the Hadamard and the CNOT gate. The Hadamard gate can be performed up to an overall phase factor as a sequence of the elementary operations \mathcal{U}_x and \mathcal{U}_z

$$\text{H} \propto \mathcal{U}_x(\theta = \frac{\pi}{4}) \mathcal{U}_z(\varphi = \frac{\pi}{4}) \mathcal{U}_x(\theta = \frac{\pi}{4}). \quad (\text{IV.63})$$

However, it also can be performed faster by simultaneous switching of B_x and B_z (compare (E.III.26), (E.III.27) and (E.IV.44)):

$$H \propto \exp\left(-i\frac{\pi}{2} \frac{\mathbf{X}+\mathbf{Z}}{\sqrt{2}}\right). \quad (\text{IV.64})$$

The CNOT operation can be implemented by a combination of two-qubit gates \mathcal{U}^{ij} (see (E.III.30)) and several single-qubit gates:

$$\begin{aligned} \text{CNOT} \propto & \mathcal{U}_x^2\left(\frac{\pi}{2}\right) \mathcal{U}_z^2\left(-\frac{\pi}{2}\right) \mathcal{U}_x^2(-\pi) \mathcal{U}^{ij}\left(-\frac{\pi}{2}\right) \\ & \times \mathcal{U}_x^1\left(-\frac{\pi}{2}\right) \mathcal{U}^{ij}\left(\frac{\pi}{2}\right) \mathcal{U}_z^1\left(-\frac{\pi}{2}\right) \mathcal{U}_z^2\left(-\frac{\pi}{2}\right). \end{aligned} \quad (\text{IV.65})$$

We see that it takes quite a number of elementary gates to perform the CNOT operation and optimization is required.

V The No-Cloning Theorem

The term *cloning* in the quantum context, coined in the short paper by **Wootters** and **Zurek**,⁸ reflects rather well the idea that there is a blueprint for quantum systems from which all its properties could be derived. However, the existence of a *Quantum Copier*, which would take one quantum system as input and produce two systems of the same kind, both of them indistinguishable from the input, is ruled out by the *no-cloning theorem*. So far, the *no-cloning theorem* has been stated only in a rather weak form, forbidding only *exact* cloning. Stronger forms give more detailed information: there is a finite error necessarily made by any putative cloner, and explicit bounds can be placed on this error.

Note that in classical systems cloning is easily possible. A special property of the classical CNOT operation is the fact that it can be used to copy bits:

$$\text{SWAP}(x,0) = (x,x). \quad (\text{V.66})$$

We can now try to use the quantum CNOT gate to make a copy of the single qubit state

$$|\Psi\rangle = a|0\rangle + b|1\rangle. \quad (\text{V.67})$$

With the two-qubit input

$$|\Psi,0\rangle = |\Psi\rangle \otimes |0\rangle = a|00\rangle + b|10\rangle \quad (\text{V.68})$$

we obtain the following output after the quantum CNOT operation

$$\text{CNOT}|\Psi,0\rangle = \text{CNOT}(a|00\rangle + b|10\rangle) = a|00\rangle + b|11\rangle. \quad (\text{V.69})$$

The copy of $|\Psi\rangle$ is however

$$|\Psi,\Psi\rangle = |\Psi\rangle \otimes |\Psi\rangle = a^2|00\rangle + b^2|11\rangle + ab|01\rangle + ab|10\rangle. \quad (\text{V.70})$$

That is,

$$\text{CNOT}|\Psi,0\rangle \neq |\Psi,\Psi\rangle. \quad (\text{V.71})$$

This result is called the *no-cloning theorem* that says that an unknown quantum state cannot be copied.

⁸W.K. Wootters and W.H. Zurek, *A single quantum cannot be cloned*, Nature **299**, 802 (1982).

VI Quantum Complexity

We have learnt that the quantum state of an n -qubit system is a vector in the 2^n dimensional Hilbert space. As an example, the state $|01001110\rangle$ is a basis vector in the 2^8 dimensional Hilbert space. In order to transform arbitrary quantum state $|\Psi\rangle$ into the new state $|\Psi'\rangle$ a unitary transformation \mathcal{U} is required:

$$|\Psi'\rangle = \mathcal{U} |\Psi\rangle, \quad (\text{VI.72})$$

where \mathcal{U} is a $2^n \times 2^n$ complex matrix. If we are dealing for example with 100 qubits, a $2^{100} \times 2^{100}$ complex matrix is required ($2^{100} \simeq 10^{30}$). This problem is called *quantum complexity*.

VII The Density Matrix Representation

The density matrix allows the calculation of the expectation values of pure and mixed quantum states. The density matrix of a quantum state is defined as

$$\hat{\rho} = |\Psi\rangle\langle\Psi|. \quad (\text{VII.73})$$

For a simple single-qubit state $|\Psi\rangle = a|0\rangle + b|1\rangle$ we obtain

$$\begin{aligned} |\Psi\rangle\langle\Psi| &= (|\Psi\rangle = a|0\rangle + b|1\rangle) \otimes (a^*\langle 0| + b^*\langle 1|) \\ &= aa^*|0\rangle\langle 0| + bb^*|1\rangle\langle 1| + ab^*|0\rangle\langle 1| + ba^*|1\rangle\langle 0| \\ &= \mathbf{P}_{00} + bb^*\mathbf{P}_{11} + ab^*\mathbf{P}_{01} + ba^*\mathbf{P}_{10} \end{aligned} \quad (\text{VII.74})$$

with the fundamental projection 2D operators

$$\mathbf{P}_{00} = |0\rangle\langle 0| = \begin{pmatrix} 1 & 0 \\ 0 & 0 \end{pmatrix} = \frac{\mathbf{1} + \mathbf{Z}}{2} \quad (\text{VII.75})$$

$$\mathbf{P}_{11} = |1\rangle\langle 1| = \begin{pmatrix} 0 & 0 \\ 0 & 1 \end{pmatrix} = \frac{\mathbf{1} - \mathbf{Z}}{2} \quad (\text{VII.76})$$

$$\mathbf{P}_{01} = |0\rangle\langle 1| = \begin{pmatrix} 0 & 0 \\ 1 & 0 \end{pmatrix} = \frac{\mathbf{X} + i\mathbf{Y}}{2} \quad (\text{VII.77})$$

$$\mathbf{P}_{10} = |1\rangle\langle 0| = \begin{pmatrix} 0 & 1 \\ 0 & 0 \end{pmatrix} = \frac{\mathbf{X} - i\mathbf{Y}}{2}. \quad (\text{VII.78})$$

Rewriting these equation we obtain the density matrix as

$$\hat{\rho} = \frac{1}{2}(\mathbf{1} + \vec{v} \cdot \vec{\sigma}) \quad (\text{VII.79})$$

with the Pauli matrices $\vec{\sigma}$ and

$$\vec{v} = \begin{pmatrix} v_x \\ v_y \\ v_z \end{pmatrix} = \begin{pmatrix} a^*b + b^*a \\ -i(a^*b - b^*a) \\ a^*a - b^*b \end{pmatrix} \quad (\text{VII.80})$$

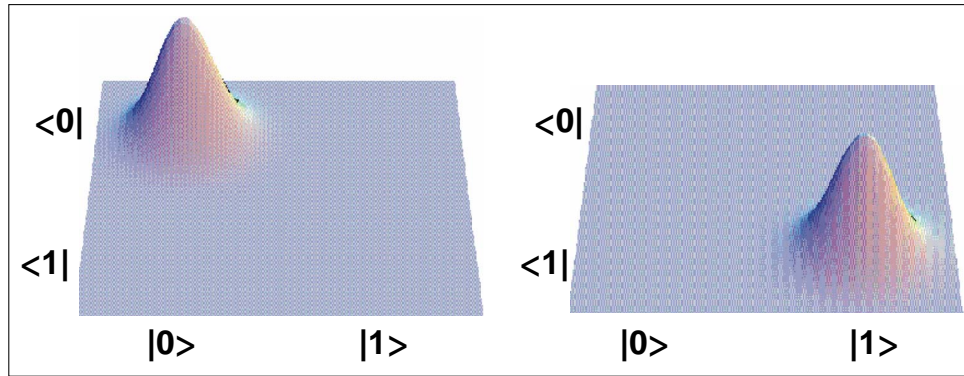


Figure E.11: Graphical representation of the density matrices $\hat{\rho}_0$ (left) and $\hat{\rho}_1$ (right) for the pure single qubit states.

For the density matrix of the pure single-qubit states we obtain

$$\hat{\rho}_0 = |0\rangle\langle 0| = \begin{pmatrix} 1 & 0 \\ 0 & 0 \end{pmatrix} \quad (\text{VII.81})$$

$$\hat{\rho}_1 = |1\rangle\langle 1| = \begin{pmatrix} 0 & 0 \\ 0 & 1 \end{pmatrix} . \quad (\text{VII.82})$$

The result is shown in Fig. E.11. We see that for the pure states there is a finite expectation value only for the respective state.

By applying the Hadamard gate we can generate a coherent superposition of the basis states (compare (E.IV.45))

$$\text{H}|0\rangle = \frac{1}{\sqrt{2}} (|0\rangle + |1\rangle) = |+\rangle \quad \text{and} \quad \text{H}|1\rangle = \frac{1}{\sqrt{2}} (|0\rangle - |1\rangle) = |-\rangle) . \quad (\text{VII.83})$$

The corresponding density matrix is

$$\begin{aligned} \hat{\rho}_+ &= \frac{1}{2} (|0\rangle + |1\rangle) \otimes (\langle 0| + \langle 1|) \\ &= \frac{1}{2} (|0\rangle\langle 0| + |0\rangle\langle 1| + |1\rangle\langle 0| + |1\rangle\langle 1|) \\ &= \frac{1}{2} \mathbf{1} + \mathbf{X} . \end{aligned} \quad (\text{VII.84})$$

The result is shown in Fig. E.12. We see that for the coherent superposition of the states achieved by the application of the Hadamard gate we obtain the same expectation value for the four possible configurations, since the Hadamard gate provides an equally weighted superposition of all basis states.

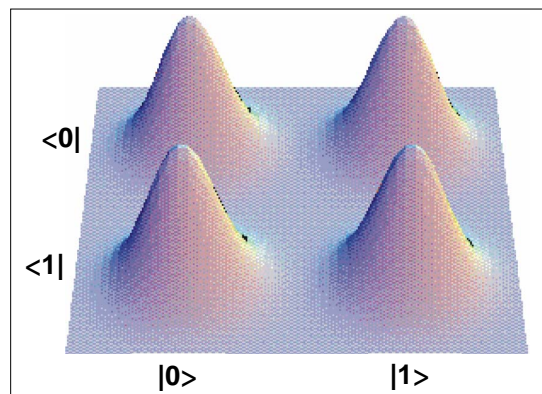


Figure E.12: Graphical representation of the density matrix $\hat{\rho}_+$ for the coherent superposition of the basis states.